ELSEVIER

Biophysical Chemistry 129 (2007) 224–234

Biophysical Chemistry

http://www.elsevier.com/locate/biophyschem

Pre-assembled clusters distort crystal nucleation kinetics in supersaturated lysozyme solutions

Avanish S. Parmar [a], Paul E. Gottschall [b], Martin Muschol [a,*]

[a] *Department of Physics, University of South Florida, Tampa, FL 33620 USA*
[b] *Department of Pharmacology & Physiology, University of South Florida, Tampa, FL 33620 USA*

Received 8 May 2007; received in revised form 4 June 2007; accepted 4 June 2007
Available online 9 June 2007

Abstract

Efficient determination of three-dimensional protein structures is critical for unraveling structure–function relationships and for supporting targeted drug design. A major impediment to these efforts is our lack of control over the nucleation and growth of high-quality protein crystals for X-ray structure determinations. While basic research on protein crystal growth mechanisms has provided valuable new insights, studies of crystal nucleation have been plagued by inconsistent and outright contradictory results. Using dynamic light scattering and SDS gel electrophoresis, we have investigated possible causes of these inconsistencies. We find that commercial sources of lyophilized hen-egg white lysozyme (HEWL) used in nucleation studies contain significant populations of large (~100 nm), pre-assembled lysozyme clusters that can readily evade standard assays of sample purity. In supersaturated solutions, these clusters act as heterogeneous nucleation centers that enhance the rate of crystal nucleation and significantly deteriorate the quality of macroscopic crystals.

Keywords: Protein crystallization; Nucleation kinetics; Protein heterogeneities; Hen egg-white lysozyme; Dynamic light scattering; Gel electrophoresis

1. Introduction

Detailed 3-dimensional protein structures provide powerful insights into the molecular mechanisms underlying the biological function of proteins [3], help to unravel the origins of many debilitating disorders [2,15,27], and support drug design targeting such disorders [1]. X-ray diffraction from high-quality protein crystals remains the most reliable approach for obtaining detailed structural information. Attempts at high-throughput protein structure determinations, however, have been frustrated by the difficulties of establishing suitable solution conditions for promoting the nucleation and subsequent growth of high-quality protein crystals. Frequently, the main bottleneck is the initial step of crystal nucleation itself [35]. The kinetics of protein crystal nucleation and the morphology of aggregates leading to crystallization *vs.* precipitation, therefore, were among the earliest targets of fundamental studies in protein crystallization [26]. A variety of experimental techniques have been used to explore protein crystal nucleation, including neutron [40] and X-ray scattering [17], video microscopy [20], nuclear magnetic resonance [14], calorimetry [9], static light scattering [28,29,52] and, most prominently, dynamic light scattering [21,24–26,32,36,53]. The results of these and other studies, however, have often remained contradictory and controversial. In addition, there is increasing evidence that protein crystal nucleation might not be well described by traditional theories of gas-liquid nucleation developed for small-molecules [30]. Hence, reliable data on the nucleation kinetics of protein crystals continue to remain essential for resolving these issues. Yet, even for the well characterized and frequently used model protein hen egg-white lysozyme, existing nucleation data disagree widely on the induction times for nucleation, nucleus sizes, or the number of critical nuclei generated under comparable solution conditions. An analysis of three recent experiments on nucleation in lysozyme using microscopy [19], microcalorimetry [9] and static light scattering [29] yielded nucleation rates that differed by as much as twenty orders of magnitude [10]. Similar disagreement exists regarding the morphology and size of

* Corresponding author. Tel.: +1 813 974 2564; fax: +1 813 974 5813.
E-mail address: mmuschol@cas.usf.edu (M. Muschol).

0301-4622/$ - see front matter © 2007 Elsevier B.V. All rights reserved.
doi:10.1016/j.bpc.2007.06.002

protein crystal nuclei. Using dynamic light scattering, Georgalis et al. [22,23,42,46] reported large populations of amorphous lysozyme clusters in supersaturated solutions. Measurements by other investigators have not been able to confirm these findings [17,38,41]. To add to the confusion, population-densities of nucleation clusters obtained from scattering techniques are often orders of magnitude larger than the number of macroscopic crystals grown under comparable solution conditions [20]. Experiments that can provide insights into the origin of these discrepancies, and how to properly address them, are a necessary first step towards future progress in this area.

Recent crystal nucleation and growth studies in our laboratory yielded similarly irreproducible results. Inconsistencies persisted even though we followed sample preparation procedures commonly used for nucleation studies (e.g. ref [11] and references therein), and in our own work [37,39]. Previous investigations of lyophilized lysozyme stock materials revealed contaminations by multiple protein impurities, which affected the growth kinetics and quality of lysozyme crystals [31,47,51]. Lorber et al. [31] correlated protein impurities (ovalbumin, BSA) in lysozyme solutions with changes in the total number and defect density of lysozyme crystals. Protein impurities have also been implicated in changes to growth rates on the 101 facet of tetragonal lysozyme crystals [12,34,50], the density of optical defects in lysozyme crystals [6] and limitations of X-ray diffraction resolution [7,33,43]. Even in the absence of contaminating impurities, structural micro-heterogeneities of lysozyme monomers have been linked to altered crystal habit and crystal quality [16]. These report, however, implicitly assumed that the contaminants were foreign proteins, or small oligomers of lysozyme. Here we report that, in addition, lyophilized lysozyme stocks contain populations of large, sub-micron clusters. These clusters are easily missed by standard protein characterization assays, and are not removed by typical sample preparation protocols used for crystal nucleation studies. We investigated the composition and physical properties of these clusters, and went on to determine their impact on the kinetics of lysozyme crystal nucleation in supersaturated solutions.

2. Materials and methods

2.1. Chemicals

Three different stock materials of lyophilized lysozyme were used: 3× recrystallized, dialyzed and lyophilized stock from Seikagaku America (cat# 100910-3, Lot LF 1121) or Sigma-Aldrich (cat# L-7651, Lot 016K11891), and 2× recrystallized, dialyzed and lyophilized stock from Worthington (cat# 2933, Lot 35E8060). All other chemicals were obtained from Fisher Scientific and were reagent grade or better.

2.2. Preparation of under- and supersaturated lysozyme solutions

Lyophilized lysozyme was dissolved directly into 0.1 M sodium acetate/ acetic acid (NaAc) buffer at pH=4.5. Prior to light scattering measurements all solutions were centrifuged at 9500 *g* for 15 min at room temperature. Lysozyme solutions were filtered either (A) through a 220 nm pore size PVDF Fisherbrand or (B) a through 20 nm pore size Anotop syringe filter. Lysozyme concentrations in solution were determined from uv absorption measured at $\lambda=280$ nm ($\alpha_{280}=2.64$ ml mg^{-1} cm^{-1} [45]).

Supersaturated solutions for nucleation and crystallization experiments were prepared by 1:1 mixing of lysozyme/buffer with NaCl/buffer stock solutions, each at twice their final concentrations. Following the method of Rosenberger et al. [44], the solubility temperature for 40 mg/ml lysozyme/4% NaCl solutions used in our nucleation studies was determined to be 39 °C. Both stock solutions were warmed to 45 °C, i.e. above the solubility of lysozyme at its final concentration, in order to dissolve any crystal seeds induced during mixing. Solutions were then transferred to preheated cuvettes and placed into the thermostated holder of our light scattering unit. Supersaturation was induced by quenching the solution temperature to 9 °C. Nucleation and growth of clusters in supersaturated solutions was investigated with three different samples: (A) Seikagaku lysozyme containing sub-micron clusters (220 nm syringe filtration) (B) Seikagaku lysozyme after removing sub-micron clusters (20 nm syringe filtration), and (C) Worthington lysozyme which was free of sub-micron clusters (therefore, 220 nm filtration was sufficient).

2.3. Dynamic light scattering (DLS) measurements

DLS measurements were performed with a Zetasizer Nano S (Malvern Instruments Ltd., UK) with a 3 mW He–Ne laser at $\lambda=633$ nm. The unit collects light back-scattered at an angle of $\theta=173°$. Sample temperature was controlled by the built-in Peltier cooling device. After thermal equilibration of the samples, autocorrelation functions were collected continuously using acquisition times of 30 s to 60 s per correlation function. Measured autocorrelation functions were converted into particle size distributions by using the "narrow modes" algorithm provided with the Zetasizer Nano S software. Particle size distributions obtained from alternative inversion algorithms yielded comparable results. A detailed discussion of the analysis of DLS data can be found elsewhere [4,8].

2.4. Thermal changes in solution viscosity

Values of buffer viscosity in the temperature range from 5 to 55 °C were derived from measurements of lysozyme diffusivity. Several precautions were taken to assure that changes in lysozyme diffusivity were not related to effects of protein interactions [37] or aggregation. Details of using proteins as tracer particles for measuring viscosity changes in aqueous media will be given in a forthcoming publication.

2.5. Separation of pre-existing clusters

Pre-existing sub-micron clusters in lysozyme stocks were separated from monomeric lysozyme or small protein

aggregates by filtering lysozyme/buffer solutions three times through 100,000 MW cutoff centrifuge filters (NanoSep 100K, Pall Corporation). After each filtration, the cluster fraction on the filter's top surface was re-dissolved into 0.5 ml NaAc buffer. Successful separation of the non-dissociated clusters from the low molecular weight protein background was confirmed using dynamic light scattering.

2.6. SDS gel electrophoresis

Aliquots of lysozyme for all three stock materials (Worthington, Seikagaku, Sigma) were analyzed either after 220 nm or 20 nm filtration with SDS PAGE gel electrophoresis. Aliquots of pre-assembled clusters isolated from Seikagaku and Sigma stock were analyzed separately. Using dynamic light scattering, we confirmed that SDS did dissociate pre-assembeld clusters into their low molecular-weight components. Protein concentrations for the cluster aliquots were below the sensitivity of our UV spectrometer (<5 μg/ml). For SDS gel electrophoresis, 15 μl of sample was mixed with 15 μl of reducing sample buffer and heated at 95 °C for 4 min, cooled and loaded onto the gel. The gel was a 12% Bis-Tris gel (Invitrogen, Carlsbad, CA) run in 3-(N-morpholino) propanesulfonic acid (MOPS) running buffer according to the manufacturers instructions. To avoid possible spill over from lanes with high protein concentrations, aliquots of dissociated Seikagaku and Sigma clusters were loaded onto lanes separated by blanks from their neighbors. Gels were stained using a high-sensitivity silver stain (Silver Snap II, Pierce). The molecular weight of markers are indicated in Fig. 3B.

2.7. Growth of macroscopic crystals

Macroscopic crystals were grown under the same conditions (including sample containers, volumes, etc) used during DLS measurements of sub-micron cluster formation. To keep the total number of macroscopic crystals at reasonable levels, the temperature–time profile for growth of macroscopic crystals had to be slightly modified: Sample temperatures were initially quenched from 45 °C to 9 °C, but solutions were kept there for only 15 min before warming them back up to room temperature (22 °C). Macroscopic crystal were then allowed to grow at room temperature overnight (16 h) before their sizes, numbers and quality were assessed.

3. Results

3.1. Detection and characterization of sub-micron clusters in undersaturated lysozyme solutions

3.1.1. Contamination of lyophilized lysozyme stock by non-dissociated sub-micron clusters

Inconsistencies in nucleation studies with hen-egg white lysozyme reported in the literature [11] and observed in our own laboratory motivated us to investigate commercial sources of hen egg white lysozyme as possible source for the observed discrepancies. Lyophilized lysozyme powder from three sources used in nucleation studies (Seikagaku America, Sigma-Aldrich, and Worthington Biochemical Corp) was directly dissolved into 100 mM sodium acetate buffer at pH=4.5 at a final concentration of 40 mg/ml (2.8 mM). Fig. 1A shows the field correlation functions of light scattered from lysozyme solutions prepared from these three stock materials. Each autocorrelation function had a rapid decay component, but solutions of Seikagaku and Sigma lysozyme also displayed a discernable "shoulder" extending to longer decay times. These slower decay times indicate the presence of aggregates. The autocorrelation functions were inverted to obtain the corresponding particle size distributions. Note that the amplitudes in these size distributions are proportional to the relative scattering intensity of the particles. To a first approximation (Rayleigh limit), this intensity

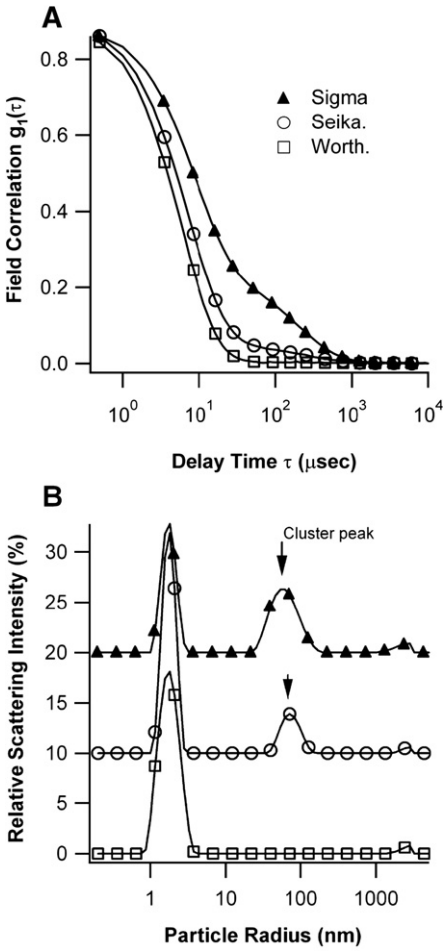

Fig. 1. Contamination of lyophilized lysozyme stock materials by sub-micron clusters. (A) Field correlation function $g_1(\tau)$ vs. delay time τ for light scattered from lysozyme solutions (C_{lys}=40 mg/ml or 2.8 mM) dissolved in 100 mM sodium acetate (NaAc) buffer at pH=4.5, T=20 °C using different lyophilized lysozyme stock: (▲) Sigma lysozyme; 3× crystallized, dialyzed, (○) Seikagaku lysozyme; 3× crystallized, dialyzed and (□) Worthington lysozyme; 2× crystallized, dialyzed. (B) Particle size distributions derived from the correlation functions shown in (A). Aside from the monomer peak located at 2 nm, notice the significant cluster peak centered near 90 nm in both Seikagaku and Sigma lysozyme samples. This sub-micron peak is completely absent from this batch of Worthington lysozyme. For clarity, the size distributions for Seikagaku and Sigma lysozyme were offset from the origin. Note: peak amplitudes are proportional to the intensity of light scattered by the particle, not their number densities.

increases with the square of the molecular weight of the cluster. Therefore, even very small fractions of large clusters yield sizeable peaks in population distributions determined with dynamic light scattering.

The particle size distributions of the unfiltered stock solutions reveal three types of well-separated peaks (Fig. 1B). The dominant peak was centered at an apparent radius of $r=(1.8\pm0.2)$ nm, consistent with the diffusivity of monomeric lysozyme under these conditions. In addition, Seikagaku and Sigma lysozyme solutions yielded pronounced cluster peaks centered around 60-90 nm. The amplitude of the cluster peak was typically larger for Sigma lysozyme, while its center was located 10–20 nm below the peak size for Seikagaku clusters. The amplitude and position of this cluster peak, however, varied somewhat with the lot number of the lysozyme stock. No such peak was detected for this batch of Worthington lysozyme (but has been found in other batches of lysozyme from the same supplier). All samples also displayed a third peak of micron-sized particles with $r=(2.3\pm0.2)$ μm, which we ascribed to air bubbles introduced during sample preparation. Sample filtration through 220 nm syringe filters and/or centrifugation readily removed this third peak. From here on out, solutions of Worthington lysozyme were only filtered through 220 nm filters since they did not contain any discernable population of pre-assembled clusters.

To confirm the size of pre-assembled clusters derived from dynamic light scattering we investigated the effects of sample filtration on particle size distributions obtained from Seikagaku stock. The autocorrelation function of the control solution (no filtration) clearly displayed the shoulder associated with the cluster peak already shown in Fig. 1. Filtration through 220 nm syringe filters and centrifugation (9500 g, 15 min) only marginally reduced the amplitude of this shoulder (Fig. 2A) and its associated cluster peak (Fig. 2B). Filtering the Seikagaku stock material through a 20 nm syringe filter completely eliminated the shoulder in the correlation function (Fig. 2A) and its associated cluster peak (Fig. 2B). Concurrently, filtration of the Seikagaku samples increased average sample diffusivity from $D=9.5\times10^{-7}$ cm^2/s for unfiltered solutions, to $D=10.9\times10^{-7}$ cm^2/s after 220 nm filtration, to over $D=12.2\times10^{-7}$ cm^2/s following 20 nm filtration. Therefore, the effects of sample filtration on the cluster peak corroborated the physical size of the clusters obtained with dynamic light scattering alone.

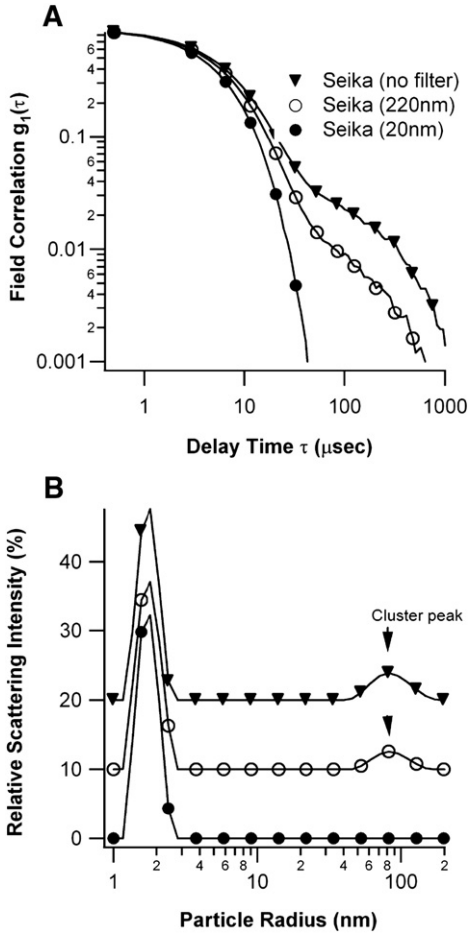

Fig. 2. Removal of sub-micron clusters by filtrations. (A) Log–log plot of field correlation function $g_1(\tau)$ for 50 mg/ml Seikagaku lysozyme in 100 mM NaAc buffer at pH=4.5 (▼) without filtration, and after filtration through a syringe filter with (○) 220 nm pore size or (●) 20 nm pore size. Notice the decline in the pronounced "shoulder" of the autocorrelation functions with decreasing filter pore size. (B) Particle size distributions derived from the correlation functions in (A). The removal of the 70–90 nm cluster peaks following 20 nm filtration support the size distributions derived from dynamic light scattering. For clarity, the size distributions for Seikagaku before and after filtration were offset from one another.

3.1.2. Analysis of cluster composition

Multiple investigators have reported contamination of lyophilized lysozyme stocks by low molecular weight (<100 kD) protein impurities [16,47,51]. We set out to determine whether the pre-assembled clusters found in lyophilized lysozyme stocks were indeed protein clusters, and which proteins they were composed of. We used 100 kD MW cut-off centrifuge filters to separate the large clusters present in Seikagaku and Sigma stock materials from protein impurities (see Materials and methods). As confirmed by dynamic light scattering, three consecutive filtrations and re-suspensions separated the cluster peak from low molecular weight proteins and aggregates (Fig. 3A). The size distributions indicated that the majority of the clusters remained intact even after repeated centrifugation and filtration, with a minor "fragment peak" appearing around 18 nm. Using DLS, we then confirmed that sodium dodecyl sulfate (SDS), completely dissociated these clusters into their low molecular weight components (data not shown).

Aliquots containing the various lysozyme stock materials were analyzed by SDS PAGE gel electrophoresis, followed by high-sensitivity silver staining (Fig. 3B). Aliquots of the isolated and SDS-dissociated cluster peak were analyzed the same way. The left hand side of the SDS gel shows the analysis of Worthington stock material after 220 nm filtration (lane A), Seikagaku lysozyme after 220 nm filtration (lane B) and 20 nm filtration (lane C), and Sigma lysozyme after 220 nm filtration (lane D) and 20 nm filtration (lane E). All lysozyme stocks contain at least three different protein contaminants with estimated molecular weights of 6, 18 and 29 kD respectively.

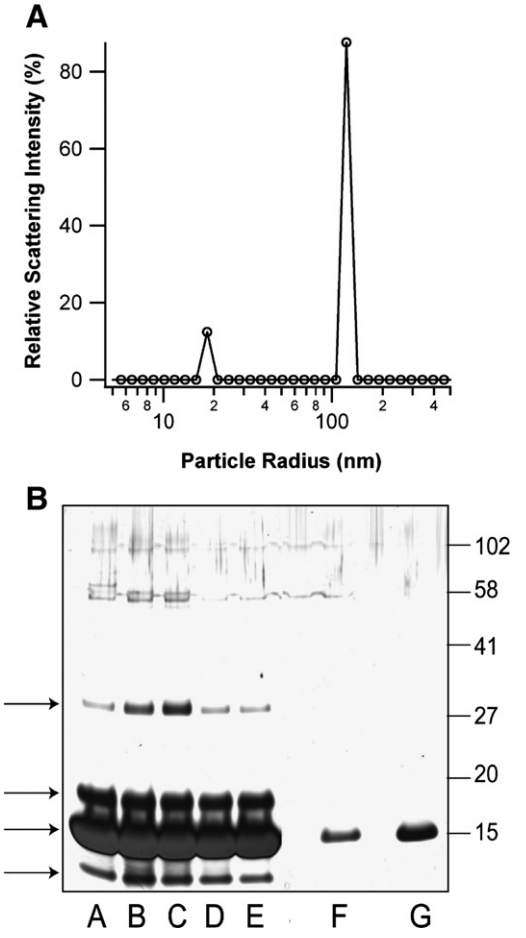

Fig. 3. SDS PAGE gel electrophoresis of lysozyme stock materials and isolated sub-micron clusters. (A) Confirmation of cluster separation: Sub-micron clusters were isolated from the stock material via repeated centrifuge filtrations. After separation, the isolated clusters were re-suspended in NaAc buffer and their size distribution determined by dynamic light scattering (for details, see Material and methods). The large peak originates from the isolated cluster population, while the small peak around 18 nm probably originates from cluster fragments generated during the repeated filtrations. (B) SDS PAGE gel electrophoresis of lysozyme stock materials (lanes A–E) and dissociated cluster fractions (lane F and G) using silver staining. Lanes: (A) Worthington lysozyme; Seikagaku lysozyme (B) with sub-micron clusters (220 nm filtration) and (C) without sub-micron clusters (20 nm filtration); Sigma lysozyme (D) with sub-micron clusters (220 nm filtration) and (E) without sub-micron clusters (20 nm filtration). Clusters peak dissociated in SDS after separation from (F) Seikagaku lysozyme and (G) Sigma lysozyme. Molecular weights of marker lanes are indicated in the right margin. The gels show bands at 6, 14, 18 and 29 kD molecular weight (see arrows at the left margin).

The 18 and 29 kD impurity bands closely match previous results by Thomas et al [51] of an unidentified impurity (18 kD) and of an SDS-resistant lysozyme dimer (28 kD). The band with the lowest molecular weight (6 kD) has not been reported before and could potentially represent a proteolytic fragment of lysozyme. As expected, filtration of Seikagaku or Sigma samples through either 220 nm or 20 nm filters had no effect on the content of low-molecular weight impurities. The analysis of the isolated and SDS-dissociated clusters from Seikagaku and Sigma stocks are shown in lane F and G of Fig. 3B. Within the resolution limit of the silver staining, the pre-assembled clusters are entirely composed of monomeric lysozyme. Notice, also, that the SDS resistant lysozyme dimers (29 kD band) do not tend to associate with these lysozyme clusters. Lysozyme stocks, therefore, contain at least three different types of heterogeneities: protein impurities, SDS-resistant lysozyme dimers, and pre-existing lysozyme clusters that can be dissociated by SDS.

3.1.3. Physical characterization of pre-existing lysozyme clusters

3.1.3.1. Concentration-dependence of protein clusters. We investigated whether the observed lysozyme clusters existed in equilibrium with their monomers or if they were non-equilibrium structures. First, we determined whether the fraction of sub-micron clusters depended on monomer concentration. Seikagaku lysozyme was dissolved in buffer solution without further purification. The relative proportion of lysozyme clusters to monomers was determined with DLS. As shown in Fig. 4, the ratio of the cluster peak area to monomer peak area was essentially independent of lysozyme concentration. Similarly, the average radius and shape of the protein cluster peak was unaffected by protein concentration. These data indicate that there is no binding-unbinding equilibrium between these lysozyme clusters and its monomers.

3.1.3.2. Thermal collapse of lysozyme clusters. We had noticed that the location of the cluster peak shifted with solution temperature. To distinguish the temperature-dependence of cluster size from thermal changes in solution viscosity, we first determined the temperature dependence of the buffer viscosity $\eta(T)$. Temperature-dependent buffer viscosity $\eta(T)$ was obtained from changes in the apparent diffusivity D_{app} of monomeric (cluster-free) lysozyme as function of lysozyme concentration C_{lys} and temperature. From the intercept of the D_{app} vs C_{lys} data we obtained $D_{0,app}$, i.e. the lysozyme diffusivity in the limit of negligible protein interactions. Using the Einstein Stokes relation, $D=k_BT/6\pi\eta r$, the temperature dependence of the buffer viscosity $\eta(T)$ was obtained. Values

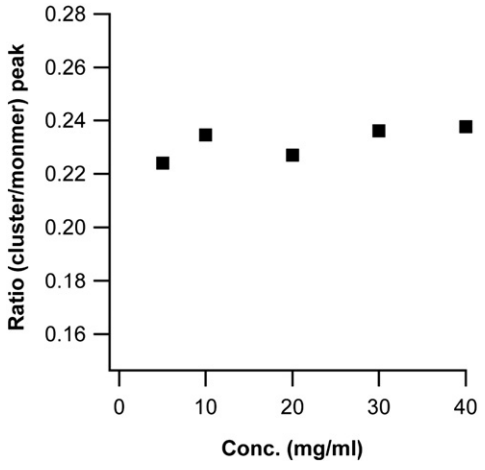

Fig. 4. Cluster population does not change with lysozyme concentration. Ratio of cluster-to-monomer peak area for unfiltered Seikagaku lysozyme in 100 mM NaAc buffer (pH=4.5) derived from dynamic light scattering measurements from lysozyme solutions at the indicated concentrations.

for the viscosity of 100 mM sodium acetate buffer thus determined fell within 3% for those of water at the same temperature and agreed with independent measurements of the dynamic viscosity of sodium acetate buffer determined at $T=20$ °C [37]. Details of these experiments and their data analysis will be presented in a forthcoming publication.

Next, we determined the changes in lysozyme cluster size in undersaturated solutions from 20 °C to 55 °C. After accounting for the temperature-dependence of buffer viscosity, $\eta(T)$, the average radius of the clusters decreased monotonically from (93 ± 5) nm at 20 °C down to (72 ± 1) nm at 55 °C (see Fig. 5). The decreasing size of the error bars in Fig. 5 indicates that the cluster size distribution became narrower with increasing temperature. When returning the solution temperature from 55 °C down to 20 °C, clusters retained their size and narrow distribution established at 55 °C, even during extended observations for 12 h (see solid square in Fig. 5).

The lack of concentration-dependent changes in cluster population and the irreversible collapse in cluster size with increasing temperature suggest that these pre-existing clusters are robust, non-equilibrium structures. This conclusion is supported by the irreversible removal of lysozyme clusters after 20 nm filtration. Given that these clusters are present in different concentrations and sizes in most stock materials, we suppose that they represent tightly bound, non-equilibrium aggregates formed to different degrees during the supplier-specific purification / lyophilization process.

3.2. Effects of sub-micron lysozyme clusters on crystal nucleation in supersaturated solutions

3.2.1. Nucleation and growth of sub-micron clusters in supersaturated lysozyme solutions

The characterization of sub-micron lysozyme clusters detailed so far has been performed in undersaturated solutions.

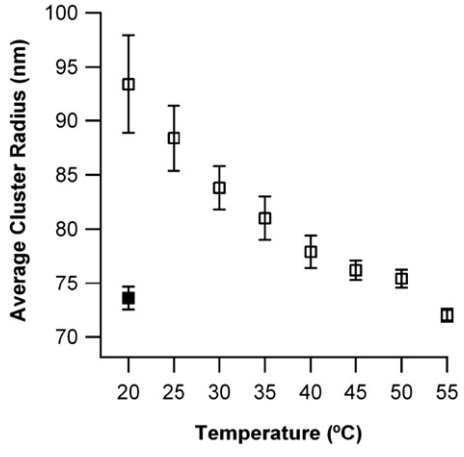

Fig. 5. Thermal collapse of sub-micron lysozyme clusters. Average cluster radius vs. solution temperature (□) in undersaturated solutions of Seikagaku lysozyme ($C_{lys}=40$ mg/ml, 100 mM NaAc, pH=4.5). The decreasing width of the error bars ($N=4$) indicates that the cluster size distribution became significantly narrower with increasing temperature. Upon cooling ($T=20$ °C) lysozyme clusters retained their size attained during heating even during extended observations over 12 h (■).

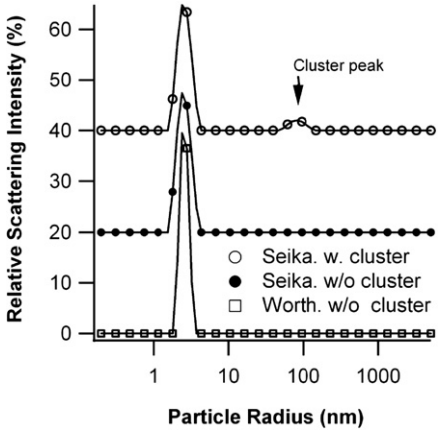

Fig. 6. Cluster distribution in lysozyme/salt solutions prior to supersaturation. Particle size distribution for Seikagaku lysozyme (○) with or (●) after removal of sub-micron clusters, and Worthington lysozyme (□) without sub-micron clusters prior to supersaturation. $C_{lys}=40$ mg/ml in 4% NaCl, 100 mM NaAc at pH=4.5, $T=45$ °C. For clarity, cluster distributions for the different samples have been offset from the origin.

Next we investigated how pre-existing lysozyme clusters affected crystal nucleation in supersaturated solutions. Since the subsequent measurements and crystallization screens required significant amount of concentrated lysozyme from a single, uniform batch, we limited these experiments to Worthington stock with no pre-existing clusters and to Seikagaku lysozyme in the presence or absence of sub-micron lysozyme clusters (see Fig. 1B).

Supersaturated lysozyme solutions at 40 mg/ml and 4% NaCl were prepared as described in the Materials and methods section. To determine the effects of pre-existing clusters on crystal nucleation kinetics, three types of stock solutions were prepared: Seikagaku lysozyme solutions were filtered either through 220 nm or 20 nm syringe filters, resulting in solutions that either did (220 nm filtration) or did not (20 nm filtration) contain pre-existing clusters. Worthington solutions, which contained no pre-existing clusters, were investigated, as well. The presence or successful removal of pre-existing clusters was established by measuring particle size distributions at 45 °C, i.e. while solutions were still undersaturated. Cluster distributions in solutions with 4% NaCl at 45 °C (Fig. 6) were essentially identical to those without NaCl obtained at the same temperature (Fig. 5). Seikagaku solutions after 220 nm filtration displayed a well developed protein cluster peak centered at 80 nm. In contrast, Seikagaku solutions after 20 nm filtrations or Worthington lysozyme after 220 nm filtration had no discernable cluster peak. The polydispersity of the Seikagaku monomer peak after cluster removal ($\delta=0.09$), however, was higher than the polydispersity of corresponding Worthington samples ($\delta=0.05$). This difference in polydispersity is consistent with the higher content of protein impurities in the Seikagaku stock (Fig. 3B, lane B or C) *vs* the Worthington stock (Fig. 3, lane A), and the presence of cluster fragments in Seikagaku samples after 20 nm filtration (Fig. 3A).

To induce supersaturation, solution temperature was quenched from 45 °C down to 9 °C, i.e. well below the solubility temperature of 39 °C. The temperature of 9 °C was

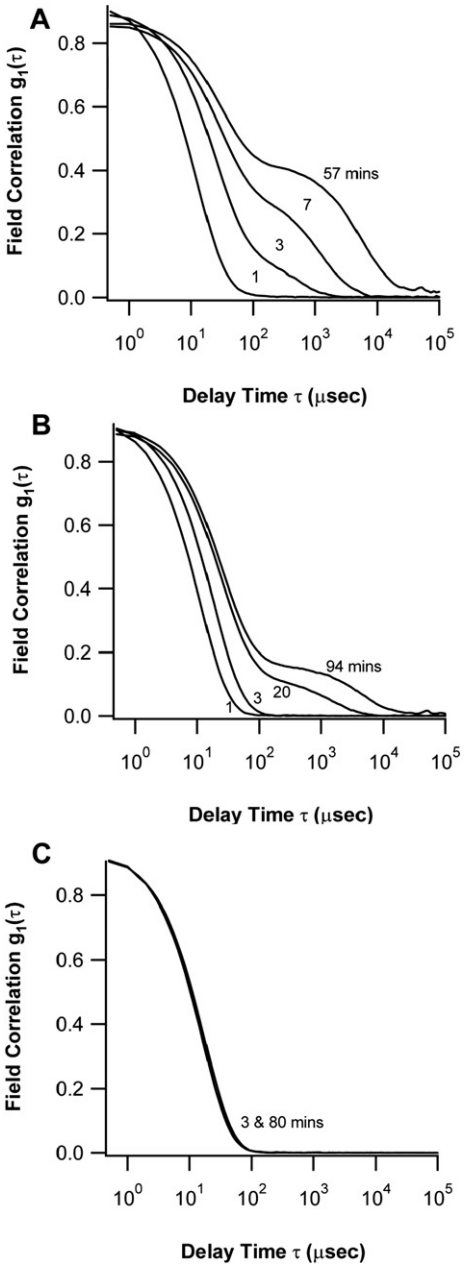

Fig. 7. Protein cluster growth in supersaturated lysozyme solutions measured with DLS. Temporal evolution of the field correlation function for light scattered from supersaturated lysozyme solutions. Data were obtained from the same solutions shown in Fig. 6, but after quenching solution temperature down to 9 °C, i.e. well below the saturation temperature of 39 °C. The correlation functions shown are those for Seikagaku lysozyme solutions (A) with pre-existing clusters or (B) without pre-existing clusters and for (C) Worthington lysozyme solution without pre-existing clusters.

chosen to accelerate crystal nucleation rates in the bulk while keeping solutions above 7 °C, the transition temperature for liquid-liquid phase separation [39]. Theoretical models [49] and experimental observations [19] have suggested that crystal nucleation rates are enhanced near this liquid-liquid phase boundary. The formation and growth of protein clusters after quenching the protein solutions into the supersaturated region is reflected in the time-dependent changes of the autocorrelation functions shown in Fig. 7. Minutes after thermal quenching, the "shoulder" of the autocorrelation function measured for Seikagaku samples with pre-existing cluster (Fig. 7A) and after removal of pre-existing cluster (Fig. 7B) started to grow in amplitude and moved towards increasingly longer decay times. Both features are indicators for the growth of significant populations of large (>50 nm) clusters in these solutions. In contrast, within the optical observation volume of our instrument (~5 nL), no cluster nucleation was discernable in the bulk of supersaturated Worthington solutions (Fig. 7C). After approx. 110 min of incubation at 9 °C, however, a drop in the zero-intercept of the autocorrelation functions developed. In all experiments, this drop in the zero-intercept coincided with the appearance of visible protein crystals at the surfaces of the sample cuvette. This is consistent with the effects of enhanced static scattering from surface-attached crystals, thereby reducing the dynamic component of light scattered from the diffusing protein particles.

Comparison of the autocorrelation functions for Seikagaku lysozyme with and Worthington without pre-existing clusters indicates that pre-existing clusters dramatically enhance the rate of new cluster nucleation and growth in supersaturated solutions. At the same time, supersaturated Seikagaku solutions after removal of large clusters via 20 nm filtration still displayed much higher cluster nucleation and growth than equivalent Worthington solutions (Fig. 7B *vs.* C). This is surprising, at first, since dynamic light scattering did not reveal a separate cluster peak in either solution (see Fig. 6). However, as noted above, Seikagaku samples after 20 nm filtration were consistently more polydisperse than the equivalent Worthington samples (δ=0.09 vs. 0.05). This implies that small-diameter aggregates (<10–20 nm) or higher impurity levels in Seikagaku samples are responsible for the pronounced difference in nucleation kinetics. It is equally noteworthy that dynamic light scattering did not detect any nucleation or growth of sub-

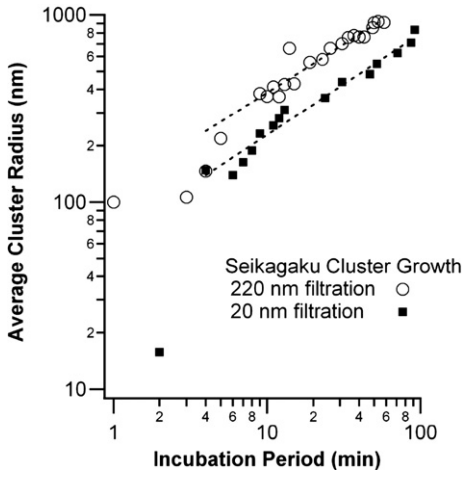

Fig. 8. Cluster growth kinetics in supersaturated lysozyme solutions. Log-log plot of the temporal evolution in cluster radius for supersaturated Seikagaku solutions (○) in the presence (■) or absence of pre-existing clusters. Cluster radii were taken from the particle size distributions obtained from dynamic light scattering. The dashed lines are fits through the data for $t \geq 5$ min with a power law for diffusion limited growth of a sphere, i.e. $r(t)=A\,t^{1/2}$.

micron cluster in the bulk of supersaturated Worthington solutions, even at these high levels of supersaturation.

3.2.2. Growth kinetics of sub-micron "nucleation" clusters

We analyzed the nucleation and growth kinetics of supersaturation-induced cluster growth in both types of Seikagaku solutions. Changes in the particle size distribution vs. incubation time in supersaturated Seikagaku solutions with or without pre-existing clusters were obtained from inversion of the dynamic light scattering data. The lysozyme monomer peak remained essentially unchanged while the average radius of the cluster peaks grew monotonically. Fig. 8 shows the temporal evolution of the average cluster radius vs. incubation time. Cluster growth in both types of Seikagaku solutions commenced without discernable delay. After a brief transition period (<3–5 min), the cluster radius increases with the square-root of incubation time (see dashed lines in Fig. 8), consistent with diffusion-limited growth of a sphere [18]. The power law, however, yielded poor fits to the critical initial stages of cluster nucleation in either sample. In this time window, cluster nucleation contributes significantly to the apparent rate of cluster growth. The temporal resolution of our dynamic light scattering measurements (~30–60 s/correlation function) was not sufficient to resolve this portion of the nucleation process.

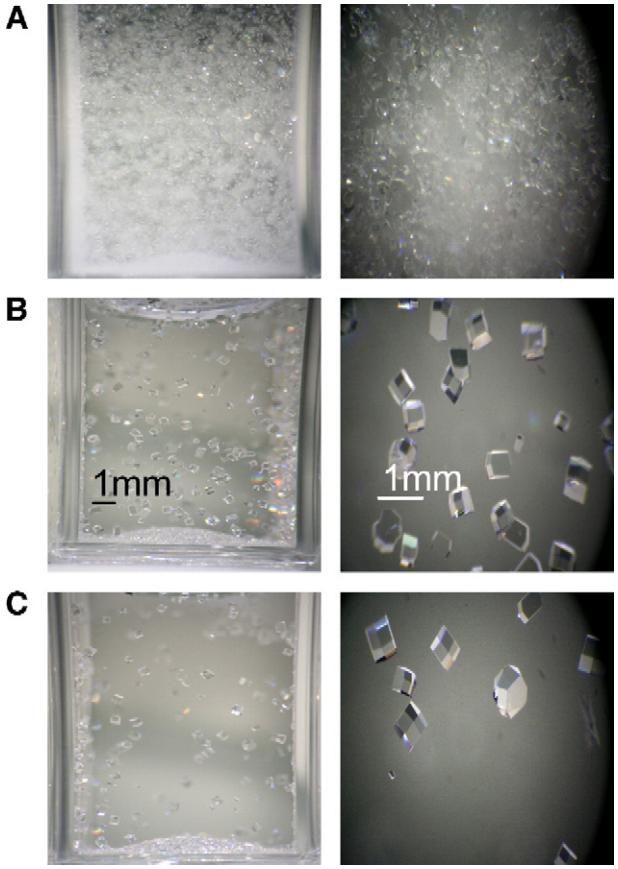

Fig. 9. Protein crystals grown from lysozyme solutions containing different levels of sub-micron clusters. *First column*: Image of the total number of crystals grown with (A) Seikagaku lysozyme with sub-micron clusters (220 nm filtration), (B) Seikagaku lysozyme after removal of sub-micron clusters (20 nm filtration) and (C) cluster-free Worthington lysozyme (220 nm filtration). *Second column*: Magnified image of tetragonal lysozyme crystals grown in each of the three cuvettes. Notice the decrease in the total number and increase in the sizes of lysozyme crystals going from top to bottom. Optical defect densities and the number of twinned crystals decreased in the same order. All solutions contained C_{lys}=40 mg/ml of lysozyme, 4% NaCl, 100 mM NaAc (pH=4.5). Lysozyme was dissolved at 45 °C, i.e. above the solubility temperature for lysozyme under these conditions. Solution temperature was quenched for 15 min to 9 °C. Solutions were then warmed back to room temperature and incubated for 16 h.

3.2.3. Effects of sub-micron lysozyme clusters on the growth of macroscopic lysozyme crystals

Fig. 9 shows typical images of macroscopic crystals grown from the three types of supersaturated lysozyme solutions investigated with dynamic light scattering for sub-micron cluster growth (Seikagaku with and after removal of pre-existing clusters, and Worthington without pre-existing clusters). As detailed in the Materials and methods section, growth conditions during macroscopic crystal growth were kept as close as possible to those used during dynamic light scattering measurements. Supersaturated solutions of Seikagaku lysozyme containing pre-existing clusters (220 nm filtration) yielded large populations of small (<0.1 mm), tetragonal crystals. These crystals were of poor optical quality and were frequently twinned. Seikagaku lysozyme without pre-existing clusters (20 nm filtration) generated far fewer macroscopic crystals of larger size (≥0.5 mm), but still with a noticeable fraction of twinned and optically defective crystals. Worthington lysozyme consistently produced the smallest number and highest quality of crystals, as ascertained by visual inspection. Since we grew crystals in the same glass cuvettes used during DLS measurements, numerical quantification of crystal numbers and defect densities between samples was not possible. Nevertheless, the results indicate that the nucleation and cluster growth behavior observed with dynamic light scattering correlates well with the outcome of macroscopic crystal growth under the same conditions: Pre-assembled lysozyme clusters dramatically increase the number of sub-micron clusters and macroscopic protein crystals, and enhance crystal defects such as twinning and optical heterogeneities.

4. Discussion

Lysozyme is a well characterized protein frequently employed for fundamental studies of protein crystal nucleation and growth. Our analysis of lyophilized lysozyme stock, commonly used without further purification in nucleation studies, indicates that commercial sources are consistently contaminated by significant populations of sub-micron (≤200 nm), non-equilibrium clusters (Fig. 1B). SDS PAGE gel chromatography of the isolated cluster fraction confirms that these large clusters are composed of lysozyme itself. Filtration through 220 nm syringe filters, the most common preparative step to eliminate large aggregates, is ineffective in removing these pre-existing clusters. In contrast to recent reports of equilibrium lysozyme clusters at high lysozyme and very low ion concentrations [48], the above lysozyme clusters are non-

equilibrium aggregates (irreversible removal by 20 nm filtration, irreversible thermal shrinking, no dependence on lysozyme concentration) already present in the lyophilized stock. Since lyophilization has been shown to induce denaturation and aggregation in a variety of proteins [5,13], we presume that lyophilization generated the pre-assembled clusters in lysozyme and that such clusters are bound to be present in many different lyophilized proteins.

In hindsight, it seems surprising that this significant sample heterogeneity has not been detected and analyzed in earlier nucleation studies. Several laboratories have carefully characterized protein impurities in lyophilized lysozyme stocks, and their impact on subsequent protein crystal growth [31,47,50,51]. Similarly, the role of structural micro-heterogeneities of lysozyme monomers was raised as possible culprit for changes in crystal growth behavior [16]. In these studies the presence of sample heterogeneities was detected using SDS PAGE gel chromatograph, size exclusion or affinity chromatography, and mass spectroscopy [42]. The sub-micron clusters reported here would have readily evaded detection by any of the above analytical techniques. These clusters are dissociated by SDS and, therefore, become part of the lysozyme monomer band in SDS gel electrophoresis (see Fig. 3B). In column chromatography, in turn, the sub-micron clusters evade UV detectors due to their low overall concentration. We were unable to obtain UV absorption readings even from aliquots highly enriched in pre-existing clusters, while those same samples yielded a well-defined cluster peak in DLS measurements (Fig. 3A).

Our dynamic light scattering measurements in supersaturated lysozyme solutions indicate that pre-existing, sub-micron lysozyme clusters have pronounced effects on the crystal nucleation and growth process. Pre-existing clusters (Seikagaku 220 nm) eliminated any discernable lag time for supersaturation-induced cluster nucleation and growth (Fig. 8A). Similar, supersaturation-induced cluster populations (Fig. 7A) and macroscopic crystal (Fig. 9A) populations were significantly enhanced by pre-existing clusters. In supersaturated solutions free of pre-existing clusters (Worthington 220 nm) no new population of nucleating lysozyme clusters were detected (Fig. 7C) even though macroscopic crystals formed on the container walls of those same samples (Fig. 9C). Non-dissociated lysozyme clusters evidently act as heterogeneous nucleation centers, promoting cluster formation in supersaturated solutions. Given the apparent affinity of lysozyme monomers for aggregation with pre-existing clusters during nucleation, non-dissociated clusters should be readily incorporated into lysozyme crystals, thereby contributing to defect formation in macroscopic crystal. This expectation is born out by the high densities of optical defects and twin boundaries observed in crystals from cluster-contaminated solutions (Fig. 9A). Both of these macroscopic defect features are bound to degrade X-ray resolution.

We originally expected that the (cluster-free) Worthington samples and the Seikagaku samples after removal of its sub-micron clusters via 20 nm filtration (Fig. 2B) would yield comparable nucleation behavior. However, the induction times for nucleation clusters emerging from supersaturated Seikagaku solutions without pre-existing clusters were closer to unfiltered Seikagaku solutions than to cluster-free Worthington solutions (see Fig. 7). Recall, though, that the polydispersity of undersaturated Seikagaku lysozyme ($\delta \approx 0.09$) was consistently higher than the polydispersity of $\delta \approx 0.05$ measured for cluster-free Worthington lysozyme solutions. Higher polydispersities imply the presence of small (<20 nm), unresolved aggregates in either solution. The higher polydispersity of "cluster-free" Seikagaku lysozyme over Worthington lysozyme could be related to two factors. As indicated by SDS PAGE gel chromatography, Seikagaku lysozyme contained higher levels of small protein impurities than Worthington lysozyme (lane A vs. lane C in Fig. 3B). Alternatively 20 nm filtration might have generated smaller cluster fragments that contributed only to the enhanced polydispersity of the "monomer peak". This latter interpretation is supported by our dynamic light scattering results from the isolated cluster peak after filtration: Besides the main cluster peak around 100 nm, the particle distributions also revealed a small secondary cluster peak centered at 18 nm (first peak, Fig. 3A), suggesting the formation of cluster fragments during filtration. In either case, the enhanced polydispersity is apparently sufficient to accelerate cluster nucleation and growth kinetics in supersaturated Seikagaku solutions. This, in turn, implies that the size of the critical nucleus for crystal formation is smaller than 20 nm.

The apparent lack of discernable cluster formation in supersaturated solutions of Worthington lysozyme deserves comment. The growth of macroscopic crystals from these solutions indicates that crystals do nucleate and grow from Worthington solutions under these conditions (Fig. 9C). To reconcile these seemingly conflicting results, note that the majority of macroscopic crystals obtained from supersaturated Worthington solutions emerged at solution interfaces, i.e. via heterogeneous surface nucleation (see, the crystals attached to the cuvette surfaces in Fig. 9). Dynamic light scattering only monitors a very small solution volume (in our instrument: 5 nL). Therefore, the absence of larger clusters from dynamic light scattering measurements suggests very low bulk nucleation rates.

The mechanisms regulating the rates, morphologies and pathways of crystal nucleation in protein solution are critical for improving our control over phase separation in macromolecular and colloidal systems, in general. While conceptually straightforward, measurements of crystal nucleation rates for proteins are fraught with experimental obstacles that have proven difficult to assess and control. Our data on lysozyme nucleation and cluster growth raise yet another experimental concern that has received little attention: sample heterogeneity due to pre-assembled protein clusters in lyophilized stock material. Two specific features of the nucleation behavior in the presence of these non-dissociated clusters are of particular concern. First, standard filtration through 0.22 μm syringe filters or centrifugation up to 15,000 g does little to remove pre-existing clusters. The presence of pre-existing clusters dramatically shortened induction times and increased the population densities of protein clusters nucleating from supersaturated solutions- two parameters that are frequently assessed for comparison with theoretical models of crystal nucleation. Pre-existing clusters

also appear to mask the intrinsic nucleation behavior of supersaturated protein solutions. Hence, contamination of lysozyme solutions by non-dissociated, non-equilibrium lysozyme clusters is a likely candidate for explaining some of the large discrepancies in nucleation rates reported in the literature [10]. Equally disconcerting are the inherent difficulties in detecting nucleation events in high-purity lysozyme samples, such as the supersaturated Worthington solutions (Fig. 7C). These observations suggest that heterogeneous surface nucleation, rather than homogeneous bulk nucleation, is the dominant pathway towards crystal seed formation in highly purified samples. Future experimental studies of protein nucleation should address these concerns.

References

[1] A.C. Anderson, The process of structure-based drug design, Chem. Biol. 10 (2003) 787–797.

[2] O. Annunziata, A. Pande, J. Pande, O. Ogun, N.H. Lubsen, G.B. Benedek, Oligomerization and phase transitions in aqueous solutions of native and truncated human bb1-crystallin, Biochemistry 44 (2005) 1316–1328.

[3] H.M. Berman, J. Westbrook, Z. Feng, G. Gilliland, T.N. Bhat, H. Weissig, I.N. Shindyalov, P.E. Bourne, The protein data bank. Nucleic Acids Res. 28 (2000) 235–242.

[4] W. Brown, Dynamic Light Scattering: The Method and Some Applications, Monographs on the Physics and Chemistry of Materials, vol. 49, Oxford University Press, New York, 1993.

[5] J.F. Carpenter, M.J. Pikal, B.S. Chang, T.W. Randolph, Rational design of stable lyophilized protein formulations: some practical advice, Pharm. Res. 14 (1997) 969–975.

[6] C.L. Caylor, I. Dobrianov, C. Kimmer, R.E. Thorne, W. Zipfel, W.W. Webb, Two-photon fluorescence imaging of impurity distributions in protein crystals, Phys. Rev. E 52 (1999) R3831–R3834.

[7] C.L. Caylor, I. Dobrianov, S.G. Lemay, C. Kimmer, S. Kriminski, K.D. Finkelstein, W. Zipfel, W.W. Webb, B.R. Thomas, A.A. Chernov, R.E. Thorne, Macromolecular impurities and disorder in protein crystals, Proteins 36 (1999) 270–281.

[8] B. Chu, Laser Light Scattering: Basic Principles and Practice, 2nd edn. Academic Press, 1991.

[9] P.A. Darcy, J.M. Wiencek, Identifying nucleation temperatures for lysozyme via differential scanning calorimetry, J. Cryst. Growth 196 (1999) 243–249.

[10] N.M. Dixit, A.M. Kulkarni, C.F. Zukoski, Comparison of experimental estimates and model predictions of protein crystal nucleation rates, Colloids Surf., A Physicochem. Eng. Asp. 190 (2001) 47–60.

[11] N.M. Dixit, C.F. Zukoski, Nucleation rates and induction times during colloidal crystallization: Links between models and experiments, Phys. Rev. E 66 (2002).

[12] P. Dolda, E. Onoa, K. Tsukamotoa, G. Sazaki, Step velocity in tetragonal lysozyme growth as a function of impurityconcentration and mass transport conditions, J. Cryst. Growth 293 (2006) 102–109.

[13] A. Dong, S.J. Prestrelski, S.D. Allison, J.F. Carpenter, Infrared spectroscopic studies of lyophilization- and temperature-induced protein aggregation. J. Pharm. Sci. 84 (1995) 415–424.

[14] J. Drenth, K. Dijkstra, C. Haas, J. Leppert, O. Ohlenschlaeger, Effect of molecular anisotropy on the nucleation of lysozyme, J. Phys. Chem. 107 (2003) 4203–4207.

[15] W.A. Eaton, J. Hofrichter, Sickle cell hemoglobin polymerization, Adv. Protein Chem. 40 (1990) 63–279.

[16] F.L. Ewing, E.L. Forsythe, M. van der Woerd, M.L. Pusey, Effects of purification of the crystallization of lysozyme, J. Cryst. Growth 160 (1996) 389–397.

[17] S. Finet, F. Bonnete, J. Frouin, K. Provost, A. Tardieu, Lysozyme crystal growth, as observed by small angle X-ray scattering, proceeds without crystallization intermediates, Eur. Biophys. J. Biophys. 27 (1998) 263–271.

[18] F.C. Frank, Radially symmetric phase growth controlled by diffusion, Proc. R. Soc. Lond. A 201 (1950) 586–599.

[19] O. Galkin, P.G. Vekilov, Are nucleation kinetics of protein crystals similar to those of liquid droplets? J. Am. Chem. Soc. 122 (2000) 156–163.

[20] O. Galkin, P.G. Vekilov, Nucleation of protein crystals: critical nuclei, phase behavior, and control pathways, J. Cryst. Growth 232 (2001) 63–76.

[21] Y. Georgalis, W. Saenger, Time-resolved light-scattering-studies on protein precrystallization fractal clusters, Adv. Colloid Interface Sci. 46 (1993) 165–183.

[22] Y. Georgalis, P. Umbach, J. Raptis, W. Saenger, Lysozyme aggregation studied by light scattering. 1. Influence of concentration and nature of electrolytes, Acta Crystallogr., D Biol. Crystallogr. 53 (1997) 691–702.

[23] Y. Georgalis, P. Umbach, W. Saenger, B. Ihmels, D.M. Soumpasis, Ordering of fractal clusters in crystallizing lysozyme solutions, J. Am. Chem. Soc. 121 (1999) 1627–1635.

[24] Y. Georgalis, P. Umbach, D.M. Soumpasis, W. Saenger, Dynamics and microstructure formation during nucleation of lysozyme solutions, J. Am. Chem. Soc. 120 (1998) 5539–5548.

[25] W. Kadima, A. McPherson, M.F. Dunn, F.A. Jurnak, Characterization of precrystallization aggregation of canavalin by dynamic light scattering, Biophys. J. 57 (1990) 125–132.

[26] Z. Kam, H.B. Shore, G. Feher, On the crystallization of proteins, J. Mol. Biol. 123 (1978) 539–555.

[27] E.H. Koo, P.T.J. Landsbury, J.W. Kelly, Amyloid diseases: abnormal protein aggregation in neurodegeneration, Proc. Natl. Acad. Sci. U. S. A. 96 (1999) 9989–9990.

[28] A. Kulkarni, C.F. Zukoski, Nanoparticle crystal nucleation: Influence of solution conditions, Langmuir 18 (2002) 3090–3099.

[29] A.M. Kulkarni, N.M. Dixit, C.F. Zukoski, Ergodic and non-ergodic phase transitions in globular protein suspensions, Faraday Discuss. 123 (2003) 37–50.

[30] A. Lomakin, N. Asherie, G.B. Benedek, Liquid–solid transition in nuclei of protein crystals, Proc. Natl. Acad. Sci. U. S. A. 100 (2003) 10254–10257.

[31] B. Lorber, M. Skouri, J.-P. Munch, R. Giege, The influence of impurities on protein crystallization: The case of lysozyme, J. Cryst. Growth 128 (1993) 1203–1211.

[32] A.J. Malkin, A. McPherson, Light scattering investigation of protein and virus crystal growth: Ferritin, apoferritin and satellite tobacco mosaic virus, J. Cryst. Growth 133 (1993) 1232–1235.

[33] A.J. Malkin, R.E. Thorne, Growth and disorder of macromolecular crystals: Insights from atomic force microscopy and X-ray divraction studies, Methods 34 (2004) 273–299.

[34] T. Matsui, G. Sazaki, H. Hondoh, Y. Matsuura, T. Nakada, K. Nakajima, Impurity effects of lysozyme molecules specifically labeled with a fluorescent reagent on the crystallization of tetragonal and monoclinic lysozyme crystals, J. Cryst. Growth 293 (2006) 415–422.

[35] A. McPherson, Crystallization of Biological Macromolecules, Cold Spring Harbor Press, 1999.

[36] V. Mikol, E. Hirsch, R. Giege, Monitoring protein crystallization by dynamic light scattering, FEBS Lett. 258 (1989) 63–66.

[37] M. Muschol, F. Rosenberger, Interactions in undersaturated and supersaturated lysozyme solutions: Static and dynamic light scattering results, J. Chem. Phys. 103 (1995) 10424–10432.

[38] M. Muschol, F. Rosenberger, Lack of evidence for prenucleation aggregate formation in lysozyme crystal growth solutions, J. Cryst. Growth 167 (1996) 738–747.

[39] M. Muschol, F. Rosenberger, Liquid–liquid phase separation in supersaturated lysozyme solutions and associated precipitate formation/crystallization, J. Chem. Phys. 107 (1997) 1953–1962.

[40] N. Niimura, Y. Minezaki, M. Ataka, T. Katsura, Aggregation in supersaturated lysozyme solution studied by time-resolved small-angle neutron-scattering, J. Cryst. Growth 154 (1995) 136–144.

[41] R. Piazza, V. Peyre, V. Degiorgio, “sticky hard spheres” model of proteins near crystallization: A test based on the osmotic compressibility of lysozyme solutions, Phys. Rev. E 58 (1998) R2733.

[42] J. Poznanski, Y. Georgalis, L. Wehr, W. Saenger, P. Zielenkiewicz, Comparison of two different lysozyme types under native and crystallization conditions using two-dimensional nmr and dynamic light scattering, Biophys. Chem. 104 (2003) 605–616.
[43] M.C. Robert, B. Capellea, B. Lorber, R. Giege, Influence of impurities on protein crystal perfection, J. Cryst. Growth 232 (2001) 489–497.
[44] F. Rosenberger, S.B. Howard, J.W. Sowers, T.A. Nyce, Temperature dependence of protein solubility- determination and application to crystallization in X-ray capillaries, J. Cryst. Growth 129 (1993) 1–12.
[45] R. Roxby, C. Tanford, Hydrogen ion titration curve of lysozyme in 6 m guanidine hydrochloride, Biochemistry 10 (1971) 3348–4.
[46] A. Schaper, Y. Georgalis, P. Umbach, J. Raptis, W. Saenger, Precrystallization structures in supersaturated lysozyme solutions studied by dynamic light scattering and scanning force microscopy, J. Chem. Phys. 106 (1997) 8587–8594.
[47] M. Skouri, B. Lorber, R. Giege, J.-P. Munch, J.S. Candau, Effect of macromolecular impurities on lysozyme solubility and crystallizability: dynamic light scattering, phase diagram and crystal growth studies, J. Cryst. Growth 152 (1995) 209–220.
[48] A. Stradner, H. Sedgwick, F. Cardinaux, W.C.K. Poon, S.U. Stefan, U. Egelhaaf, P. Schurtenberger, Equilibrium cluster formation in concentrated protein solutions and colloids, Science 435 (2004) 492–495.
[49] P.R. tenWolde, D. Frenkel, Enhancement of protein crystal nucleation by critical density fluctuations, Science 277 (1997) 1975–1978.
[50] B.R. Thomas, P.G. Vekilov, F. Rosenberger, Effects of microheterogeneity on hen egg white lysozyme crystallization, Acta Crystallogr., D Biol. Crystallogr. 54 (1998) 226–236.
[51] B.R. Thomas, P.G. Vekilov, F. Rosenberger, Heterogeneity determination and purification of commercial hen egg-white lysozyme, Acta Crystallogr., D Biol. Crystallogr. 52 (1996) 776–784.
[52] J.L. Wilson, M.L. Pusey, Determination of monomer concentrations in crystallizing lysozyme solutions, J. Cryst. Growth 122 (1992) 8–13.
[53] W.W. Wilson, Monitoring crystallization experiments using dynamic light scattering: Assaying and monitoring protein crystallization in solution, Method 1 (1990) 110–117.